

Quantum theory of the maser. I. General theory

Georg M. Meyer,^{1,2,3} Marlan O. Scully,^{1,2} and Herbert Walther^{1,3}

¹Max-Planck-Institut für Quantenoptik, Hans-Kopfermann-Strasse 1, D-85748 Garching, Germany

²Department of Physics, Texas A&M University, College Station, Texas 77843

and Texas Laser Laboratory, Houston Advanced Research Center, The Woodlands, Texas 77381

³Sektion Physik, Ludwig-Maximilians-Universität, München, Germany

(Received 9 April 1997)

The photon emission probability in a micromaser changes drastically when the kinetic energy of the pumping atoms is comparable to the atom-field interaction energy. In this situation, the atomic center-of-mass motion has to be treated quantum mechanically and the de Broglie wavelength of the atom inside the cavity is an important physical parameter. The interplay between reflection and transmission of the atoms leads to a new mechanism for induced emission. A photon is emitted by an excited atom when the de Broglie wavelength fits resonantly into the cavity. These resonances lead to the process of microwave amplification via z -motion-induced emission of radiation (maser). We derive and illustrate a general expression for the emission probability and a master equation for the maser. We note that the probability for emission by an excited thermal atom (stimulated maser emission) is very different from the emission probability as given by the de Broglie resonances (induced maser emission). [S1050-2947(97)01411-X]

PACS number(s): 42.50.Ar, 32.80.-t, 42.50.Dv, 84.40.Ik

I. INTRODUCTION

Maser action occurs when excited thermal atoms follow classical trajectories through a cavity [1–5]. We have shown recently [6] that operation in the limit of ultracold (laser-cooled) atoms [7] requiring a quantum-mechanical treatment of the center-of-mass (CM) motion [8,9] leads to a completely new kind of induced emission. In the ordinary maser, stimulated emission prevails as the mechanism for amplification of radiation; but in the case of ultracold atoms the physics of the induced emission process is intimately associated with the quantization of the CM motion (taken to be in the z direction). For this reason we distinguish between the usual stimulated emission maser physics and that characterized by the present quantized- z -motion-induced emission, and call the process of microwave amplification via z -motion-induced emission of radiation the maser action.

The physical mechanism responsible for the induced emission is the longitudinal force that the atoms experience upon passing into a high- Q cavity due to the abrupt change in the atom-field interaction. Different dressed-state components of the combined atom-field system encounter different potentials and experience different longitudinal forces. The different reflection and transmission of the dressed-state components may result in the emission of a photon.

In this paper we study in detail the quantized- z -motion-induced emission and the photon statistics of the micromaser pumped by slow atoms. In Sec. II we show that the interaction of slow atoms with a cavity field can be viewed as a scattering problem. In Sec. III we give a general expression for the emission probability of an excited atom that is incident upon a cavity with n photons. In order to study the cumulative effect of a sequence of incident atoms on the cavity field, we derive in Sec. IV a master equation for the field. In the following we first study the case where the atom-field coupling strength inside the cavity is constant along the propagation axis of the atoms. This situation can be

treated analytically and describes a TM mode. In Sec. V the emission probability for the incident atoms and the photon statistics of the cavity field are studied in detail. We distinguish three very different cases that we call the Rabi regime, the intermediate regime, and the maser regime: the kinetic energy of the atoms is larger than, on the order of, or smaller than the atom-field interaction energy, respectively. The resonances that occur in the maser limit for very slow atoms are explained in Sec. VI in terms of the reflection and transmission of dressed-state components and by looking at the de Broglie wavelength of the atoms inside the cavity. A sinusoidal mode function, which corresponds to a TE mode, is considered in Sec. VII. In conclusion, we summarize our main results. A discussion of more general mode functions and possible experimental realizations will be given in paper II, spectral properties are considered in paper III of this series [10,11].

II. ATOM-FIELD INTERACTION AS A SCATTERING PROBLEM

We first study the interaction between an incident atom in the excited state $|a\rangle$ and a cavity field with n photons, taking the quantum-mechanical CM motion of the atom into account. With the atomic lowering (raising) operator $\sigma = |b\rangle\langle a|$ ($\sigma^\dagger = |a\rangle\langle b|$), the cavity-field annihilation (creation) operator a (a^\dagger), and the CM momentum operator p_z , the atom-field Hamilton operator reads in the dipole and rotating-wave approximation

$$H = \hbar \nu_c a^\dagger a + \hbar \omega \sigma^\dagger \sigma + \frac{p_z^2}{2M} + \hbar g u(z) (\sigma a^\dagger + a \sigma^\dagger), \quad (1)$$

where $u(z)$ is the mode function of the cavity field, g is the atom-field coupling strength for the interaction between the quantized field (with frequency ν_c) and the atom (with level

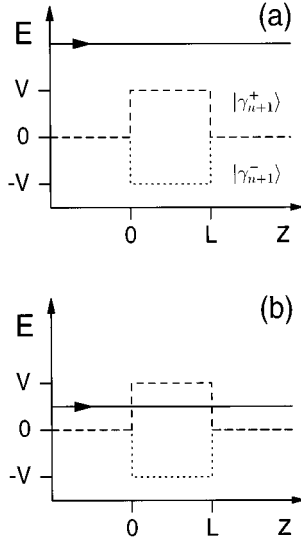


FIG. 1. Schematic representation of the energy E of the atoms (solid line) incident upon a micromaser cavity of length L , which acts as a repulsive potential or potential barrier (dashed) and as an attractive potential (dotted) with a potential energy $V = \hbar g \sqrt{n+1}$ for a cavity with n photons.

spacing $\hbar\omega$), and M is the atomic mass. For simplicity, we assume the atom to be in resonance with the field, i.e., $\nu_c = \omega$.

In an interaction picture, using a reference frame that eliminates the terms in Eq. (1) that correspond to the energy of the free field and the internal energy of the free atom, we have the Hamilton operator

$$\tilde{H} = \frac{p_z^2}{2M} + \hbar g u(z) (\sigma a^\dagger + a \sigma^\dagger). \quad (2)$$

It is expedient to expand the atom-field state in terms of the dressed states

$$|\gamma_{n+1}^\pm\rangle = \frac{1}{\sqrt{2}} (|a, n\rangle \pm |b, n+1\rangle), \quad (3)$$

which are the eigenstates of the interaction operator, i.e.,

$$(\sigma a^\dagger + a \sigma^\dagger) |\gamma_{n+1}^\pm\rangle = \pm \sqrt{n+1} |\gamma_{n+1}^\pm\rangle. \quad (4)$$

As discussed in Ref. [8], Eqs. (2) and (4) lead to the elementary problem of a particle incident upon a potential $V_n^\pm(z) = \pm \hbar g \sqrt{n+1} u(z)$, as sketched in Fig. 1. When an atom in the excited state $|a\rangle$ and with a CM wave packet $\psi(z)$ is incident upon a cavity field in the number state $|n\rangle$, the atom-field system is characterized before the scattering process by the wave function

$$\langle z | \Psi(0) \rangle = \psi(z, 0) |a, n\rangle \quad (5)$$

with

$$\psi(z, 0) = \int dk A(k) e^{ikz} \theta(-z). \quad (6)$$

Here Heaviside's unit step function θ merely indicates on which side of the cavity the atom can be found; of course, the position and extent of the wave packet are already determined by the amplitudes $A(k)$.

Inserting $|a, n\rangle = (|\gamma_{n+1}^+\rangle + |\gamma_{n+1}^-\rangle) / \sqrt{2}$ into Eq. (5), we express the initial state as a sum of components of the form

$$\Psi_n^\pm(z, 0) = \psi(z, 0) |\gamma_{n+1}^\pm\rangle, \quad (7)$$

each of which obeys the time-dependent Schrödinger equation

$$i\hbar \frac{\partial}{\partial t} \Psi_n^\pm(z, t) = \left(-\frac{\hbar^2}{2M} \frac{\partial^2}{\partial z^2} + V_n^\pm(z) \right) \Psi_n^\pm(z, t). \quad (8)$$

That is, each Ψ_n^+ component encounters the potential $V_n^+(z)$ and each Ψ_n^- component sees the potential $V_n^-(z)$. We have thus reduced the problem to an elementary scattering process and denote the reflection and transmission coefficients for the Ψ_n^\pm components by ρ_n^\pm and τ_n^\pm , respectively.

After the atom has left the interaction region, the initial state (5) has evolved into

$$\begin{aligned} \langle z | \Psi(t) \rangle &= \frac{1}{\sqrt{2}} \int dk A(k) e^{-i(\hbar k^2/2M)t} \{ [\rho_n^+(k) e^{-ikz} \theta(-z) \\ &\quad + \tau_n^+(k) e^{ik(z-L)} \theta(z-L)] |\gamma_{n+1}^+\rangle \\ &\quad + [\rho_n^-(k) e^{-ikz} \theta(-z) \\ &\quad + \tau_n^-(k) e^{ik(z-L)} \theta(z-L)] |\gamma_{n+1}^-\rangle \} \\ &= \int dk A(k) e^{-i(\hbar k^2/2M)t} [R_{an}(k) e^{-ikz} \theta(-z) |a, n\rangle \\ &\quad + T_{an}(k) e^{ik(z-L)} \theta(z-L) |a, n\rangle \\ &\quad + R_{b, n+1}(k) e^{-ikz} \theta(-z) |b, n+1\rangle \\ &\quad + T_{b, n+1}(k) e^{ik(z-L)} \theta(z-L) |b, n+1\rangle]. \quad (9) \end{aligned}$$

An excited atom incident upon a cavity that contains n photons is found to be reflected or transmitted while remaining in the excited state $|a\rangle$ with amplitudes

$$R_{an} = \frac{1}{2} (\rho_n^+ + \rho_n^-), \quad (10)$$

$$T_{an} = \frac{1}{2} (\tau_n^+ + \tau_n^-)$$

and is similarly reflected or transmitted while making a transition to the state $|b\rangle$, and emitting a photon, with amplitudes

$$R_{b, n+1} = \frac{1}{2} (\rho_n^+ - \rho_n^-), \quad (11)$$

$$T_{b, n+1} = \frac{1}{2} (\tau_n^+ - \tau_n^-).$$

These four cases are sketched in Fig. 2.

III. EMISSION PROBABILITY

From Eq. (11), we obtain a general expression for the probability that an excited atom incident upon a cavity containing n photons will emit a photon:

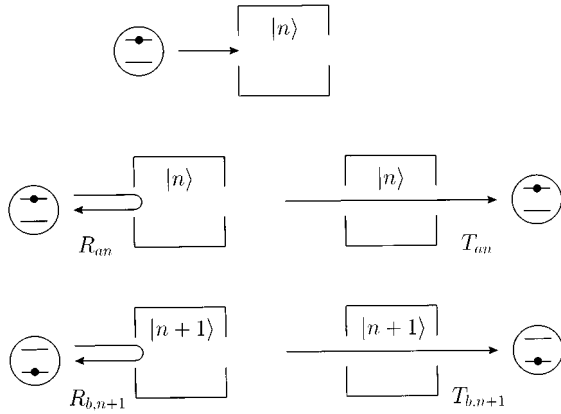


FIG. 2. An excited atom incident upon a cavity that contains n photons is reflected or transmitted and remains in the excited state or deposits a photon in the cavity with probability amplitudes R_{an} , T_{an} , $R_{b,n+1}$, and $T_{b,n+1}$.

$$P_{\text{emission}}(n) = |R_{b,n+1}|^2 + |T_{b,n+1}|^2 \\ = \frac{1}{4} (|\rho_n^+ - \rho_n^-|^2 + |\tau_n^+ - \tau_n^-|^2). \quad (12)$$

The emission probability depends therefore only on the reflection and transmission coefficients for the quantum-mechanical CM motion of the atom. For very slow atoms the reflection coefficients do not vanish, and the emission probability changes drastically. This is the reason why the new kind of induced emission is called quantized-motion-induced emission.

In the special case where the atom-field coupling inside the cavity is constant along the propagation axis of the atoms, the reflection and transmission coefficients can be calculated analytically. The mode function is then given by the mesa function

$$u(z) = \begin{cases} 1 & \text{for } 0 < z < L \\ 0 & \text{elsewhere,} \end{cases} \quad (13)$$

where L is the length of the cavity in the z direction. In this case, each Ψ_n^+ component encounters a potential barrier and each Ψ_n^- component sees a square-well potential. This is shown schematically in Fig. 1. We obtain for the mesa function the reflection and transmission coefficients

$$\rho_n^\pm = i\Delta_n^\pm \sin(k_n^\pm L) \tau_n^\pm, \\ \tau_n^\pm = [\cos(k_n^\pm L) - i\Sigma_n^\pm \sin(k_n^\pm L)]^{-1}, \quad (14)$$

where

$$k_n^\pm = (k^2 \mp \kappa^2 \sqrt{n+1})^{1/2}, \\ \Delta_n^\pm = \frac{1}{2} \left(\frac{k_n^\pm}{k} - \frac{k}{k_n^\pm} \right), \\ \Sigma_n^\pm = \frac{1}{2} \left(\frac{k_n^\pm}{k} + \frac{k}{k_n^\pm} \right), \quad (15)$$

$\hbar k$ is the atomic CM momentum, and $(\hbar \kappa)^2/2M = \hbar g$ is the vacuum coupling energy. For the emission probability, we obtain in general from Eqs. (12) and (14)

$$P_{\text{emission}}(n) \\ = \frac{1}{2} \left[1 - \frac{(1 + \Delta_n^+ \Delta_n^- S_n^+ S_n^-)(C_n^+ C_n^- + \Sigma_n^+ \Sigma_n^- S_n^+ S_n^-)}{(C_n^{+2} + \Sigma_n^{+2} S_n^{+2})(C_n^{-2} + \Sigma_n^{-2} S_n^{-2})} \right] \quad (16)$$

with $C_n^\pm = \cos(k_n^\pm L)$ and $S_n^\pm = \sin(k_n^\pm L)$. In Sec. V we will discuss the emission probability in detail and derive simpler formulas for limiting cases.

For the mesa mode and thermal atoms, the atomic momentum inside the cavity is

$$\hbar k_n^\pm = \hbar k \left(1 \mp \frac{\kappa_n^2}{2k^2} \right), \quad (17)$$

with $\kappa_n = \kappa \sqrt{n+1}$; that is, the atoms that experience the potential well are faster and the atoms that see a repulsive potential are slower inside the cavity. Therefore, the wave function (9) after the atom-field interaction reduces to the form

$$\langle z | \Psi(t) \rangle = \psi(z, t) \frac{1}{\sqrt{2}} [\exp(-i\kappa_n^2 L/2k) |\gamma_{n+1}^+\rangle \\ + \exp(i\kappa_n^2 L/2k) |\gamma_{n+1}^-\rangle] \\ = \psi(z, t) [\cos(g\tau\sqrt{n+1}) |a, n\rangle \\ - i\sin(g\tau\sqrt{n+1}) |b, n+1\rangle] \quad (18)$$

with

$$\psi(z, t) = \int dk A(k) e^{ikz} \theta(z-L) e^{-i(\hbar k^2/2M)t} \quad (19)$$

and $g\tau = \kappa^2 L/2k$. We have thus recovered the well-known Rabi oscillations.

When the cavity mode is not described by a mesa function, the coefficients (14) are modified. However, Eqs. (10), (11), and (12) still hold.

IV. DERIVATION OF THE MASTER EQUATION

We now consider a more general situation where the two-level atom is in the state $c_a|a\rangle + c_b|b\rangle$ and the cavity field is in the state $\sum_n c_n |n\rangle$. The atom-field system is now characterized before the scattering process by the wave function

$$\langle z | \Psi(0) \rangle = \psi(z, 0) \sum_{n=0}^{\infty} (c_{an} |a, n\rangle + c_{bn} |b, n\rangle) \quad (20)$$

with $c_{an} = c_a c_n$ and $c_{bn} = c_b c_n$. Expanding $|a, n\rangle$ and $|b, n+1\rangle$ in terms of dressed states, we obtain in the same way as in Sec. II the state of the atom-field system after the interaction

$$\langle z | \Psi(t) \rangle = \int dk A(k) e^{-i(\hbar k^2/2M)t} \left\{ c_{b0} e^{ikz} \theta(z-L) |b, 0\rangle \right. \\ \left. + \sum_{n=0}^{\infty} [\mathcal{R}_{an}(k) e^{-ikz} \theta(-z) |a, n\rangle \right.$$

$$\begin{aligned}
& + \mathcal{T}_{an}(k)e^{ik(z-L)}\theta(z-L)|a,n\rangle \\
& + \mathcal{R}_{b,n+1}(k)e^{-ikz}\theta(-z)|b,n+1\rangle \\
& + \mathcal{T}_{b,n+1}(k)e^{ik(z-L)}\theta(z-L)|b,n+1\rangle \Big\}, \quad (21)
\end{aligned}$$

where

$$\mathcal{R}_{an} = c_{an}R_{an} + c_{b,n+1}R_{b,n+1}, \quad (22)$$

$$\mathcal{T}_{an} = c_{an}T_{an} + c_{b,n+1}T_{b,n+1}$$

are the probability amplitudes for finding the atom reflected or transmitted in the upper state and n photons in the cavity field and

$$\mathcal{R}_{b,n+1} = c_{an}R_{b,n+1} + c_{b,n+1}R_{an}, \quad (23)$$

$$\mathcal{T}_{b,n+1} = c_{an}T_{b,n+1} + c_{b,n+1}T_{an}$$

are the amplitudes for finding the atom reflected or transmitted in the lower state and $n+1$ photons in the field. In the special case treated in Sec. II, we have $c_a=1$ and $c_n=1$ for a fixed value of n , and therefore $\mathcal{R}_{an}=R_{an}$, $\mathcal{T}_{an}=T_{an}$, $\mathcal{R}_{b,n+1}=R_{b,n+1}$, and $\mathcal{T}_{b,n+1}=T_{b,n+1}$.

Please note that R_{an} is not only the probability amplitude for an atom in the upper state $|a\rangle$ to be reflected and to remain in $|a\rangle$, but also for an atom in the lower state $|b\rangle$ to be reflected and to remain in $|b\rangle$; and $R_{b,n+1}$ is not only the probability amplitude for an atom in state $|a\rangle$ to be reflected and to undergo a transition to $|b\rangle$, but also for an atom in $|b\rangle$ to make a transition to $|a\rangle$. Analogously, T_{an} should be understood as the probability amplitude for an incident atom (in $|a\rangle$ or $|b\rangle$) to be transmitted without undergoing a transition, and $T_{b,n+1}$ is the amplitude for an atom to be transmitted with a transition taking place.

Equation (21) can be used to find the reduced density matrix $\rho(t)$ for the cavity field after the interaction with the excited atom by forming the atom-field density matrix and tracing over the internal and external atomic degrees of freedom, that is,

$$\rho(t) = \sum_{i=a,b} \int dz \langle i,z | \Psi(t) \rangle \langle \Psi(t) | i,z \rangle. \quad (24)$$

The coarse-grained equation of motion for the radiation field is then given by

$$\dot{\rho}(t) = r\delta\rho(t) + L\rho(t), \quad (25)$$

where r is the atomic injection (or incidence) rate and $\delta\rho(t)$ is the change in the reduced density matrix of the field due to the interaction with a single atom in the state

$$\varrho_{\text{atom}} = \sum_{i,j=a,b} \varrho_{ij} |i\rangle\langle j| \quad \text{with } \varrho_{ij} = c_i c_j^*. \quad (26)$$

Field damping is described by the Liouville operator

$$\begin{aligned}
L\rho = & -\frac{C}{2}(n_b+1)(a^\dagger a \rho + \rho a^\dagger a - 2a \rho a^\dagger) \\
& -\frac{C}{2}n_b(aa^\dagger \rho + \rho aa^\dagger - 2a^\dagger \rho a), \quad (27)
\end{aligned}$$

where C is the cavity decay rate and n_b is the number of photons in thermal equilibrium. We have neglected the dissipation during the atom-field interaction [12].

Inserting Eq. (21) into (24) and adding the terms describing field damping, we find the equations of motion for the density-matrix elements

$$\begin{aligned}
\dot{\rho}_{nn'} = & [r\varrho_{aa}(R_{an}R_{an}^* + T_{an}T_{an}^* - 1) + r\varrho_{bb}(R_{a,n-1}R_{a,n-1}^* + T_{a,n-1}T_{a,n-1}^* - 1)]\rho_{nn'} \\
& + r\varrho_{aa}(R_{bn}R_{bn}^* + T_{bn}T_{bn}^*)\rho_{n-1,n'-1} + r\varrho_{bb}(R_{b,n+1}R_{b,n+1}^* + T_{b,n+1}T_{b,n+1}^*)\rho_{n+1,n'+1} \\
& + r\varrho_{ab}[(R_{an}R_{b,n'+1}^* + T_{an}T_{b,n'+1}^*)\rho_{n,n'+1} + (R_{bn}R_{a,n'-1}^* + T_{bn}T_{a,n'-1}^*)\rho_{n-1,n'}] \\
& + r\varrho_{ba}[(R_{b,n+1}R_{an}^* + T_{b,n+1}T_{an}^*)\rho_{n+1,n'} + (R_{a,n-1}R_{bn}^* + T_{a,n-1}T_{bn}^*)\rho_{n,n'-1}] \\
& - \frac{1}{2}C(n_b+1)[(n+n')\rho_{nn'} - 2\sqrt{(n+1)(n'+1)}\rho_{n+1,n'+1}] \\
& - \frac{1}{2}Cn_b[(n+n'+2)\rho_{nn'} - 2\sqrt{nn'}\rho_{n-1,n'-1}]. \quad (28)
\end{aligned}$$

In the following we will restrict ourselves to the injection of excited atoms ($\varrho_{aa} = 1$). In this case, Eq. (28) simplifies to

$$\begin{aligned} \dot{\rho}_{nn'} = & r(R_{an}R_{an'}^* + T_{an}T_{an'}^* - 1)\rho_{nn'} \\ & + r(R_{bn}R_{bn'}^* + T_{bn}T_{bn'}^*)\rho_{n-1,n'-1} \\ & - \frac{1}{2}C(n_b+1)[(n+n')\rho_{nn'} \\ & - 2\sqrt{(n+1)(n'+1)}\rho_{n+1,n'+1}] \\ & - \frac{1}{2}Cn_b[(n+n'+2)\rho_{nn'} - 2\sqrt{nn'}\rho_{n-1,n'-1}]. \end{aligned} \quad (29)$$

V. PHOTON STATISTICS

The equation of motion for the photon-number distribution $P(n) = \rho_{nn}$ follows from Eq. (29):

$$\begin{aligned} \dot{P}(n) = & G_{n-1}P(n-1) - G_nP(n) \\ & - C(n_b+1)[nP(n) - (n+1)P(n+1)] \\ & + Cn_b[nP(n-1) - (n+1)P(n)], \end{aligned} \quad (30)$$

where $G_n = rP_{\text{emission}}(n)$ is the gain coefficient with the emission probability P_{emission} as in Eq. (12).

The rate of change of the mean number of photons

$$\langle \dot{n} \rangle = \langle G_n \rangle - C(\langle n \rangle - n_b) \quad (31)$$

and the steady-state photon distribution

$$P(n) = P(0) \prod_{m=1}^n \frac{Cn_b + G_{m-1}/m}{C(n_b+1)} \quad (32)$$

follow from Eq. (30). The photon distribution of the mazer pumped by ultracold atoms is completely different from the field in the micromaser operating with a beam of thermal atoms.

The difference between the classical and the quantum treatment of the CM motion is clearly illustrated by looking at the probability that an excited atom launched into a cavity containing n photons will emit a photon. As we have seen in Sec. III, this emission probability $P_{\text{emission}}(n)$ depends on the relation between the kinetic energy of the atoms and the atom-field interaction energy. We distinguish the situations where the kinetic energy of the atoms is larger than, on the order of, or smaller than the atom-field coupling energy and call these cases the Rabi regime, the intermediate regime, and the mazer regime, respectively. The emission probability is qualitatively different in these regimes. This is illustrated in Fig. 3 for $k/\kappa = 10, 1, 0.1,$ and 0.01 , when the cavity field is initially in the vacuum state ($n = 0$). Please note that in the Rabi regime the emission probability is periodic in $g\tau\sqrt{n+1}$, in the mazer regime it is periodic in $\kappa L\sqrt[4]{n+1}$. This difference in the scaling parameter will be discussed in the next subsections.

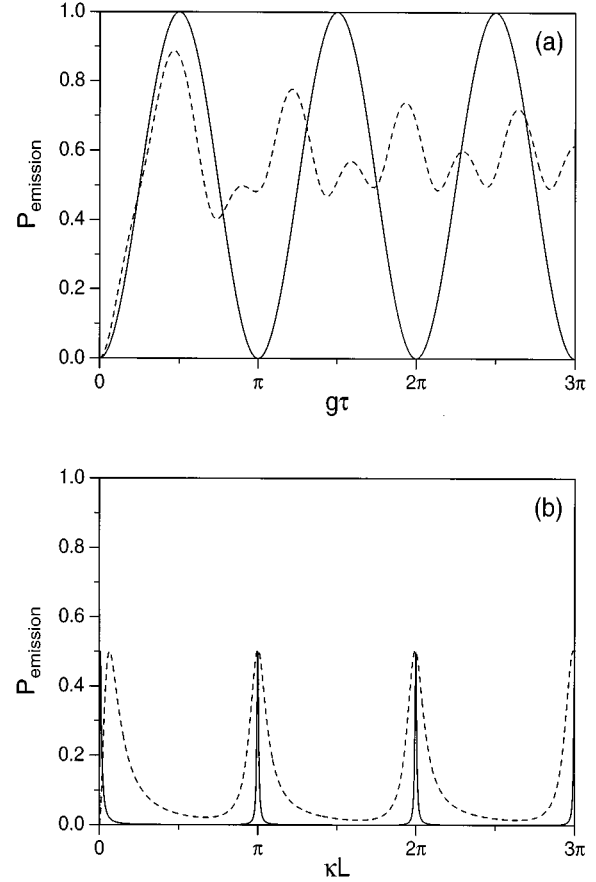


FIG. 3. The emission probability P_{emission} vs the interaction time $g\tau$ (a) for fast atoms with $k/\kappa = 10$ (solid) and $k/\kappa = 1$ (dashed) and vs the interaction length κL (b) for slow atoms with $k/\kappa = 0.01$ (solid) and $k/\kappa = 0.1$ (dashed), when the cavity field is initially in the vacuum state. As indicated by the dashed curve in (b), an increase in the velocity of ultracold atoms results in a broadening of the resonances.

A. Rabi limit

For fast atoms with $k \gg \kappa_n = \kappa\sqrt[4]{n+1}$, the emission probability is given by

$$P_{\text{emission}}(n) = \sin^2\left(\frac{\kappa^2 L}{2k}\sqrt{n+1}\right). \quad (33)$$

Equation (33) embodies the usual stimulated emission process and the well-known Rabi oscillations. For example, when L is small so that $(\kappa^2 L/2k)\sqrt{n+1} = \Omega_n \tau \ll 1$, where the Rabi frequency $\Omega_n = g\sqrt{n+1}$ and the interaction time $\tau = L(\hbar k/M)^{-1}$, then the emission probability is proportional to $n+1$.

The influence of the potential barrier on the photon statistics can be observed even if the kinetic energy of the atoms is larger than the atom-field interaction energy. For example, the trapping resonances [13] of the conventional micromaser, which can be found at very low temperatures, i.e., in the absence of thermal photons, begin to disappear when the atoms are cooled down so that $k \approx 10\kappa$ (for $r/C = 50$). This is illustrated in Fig. 4.

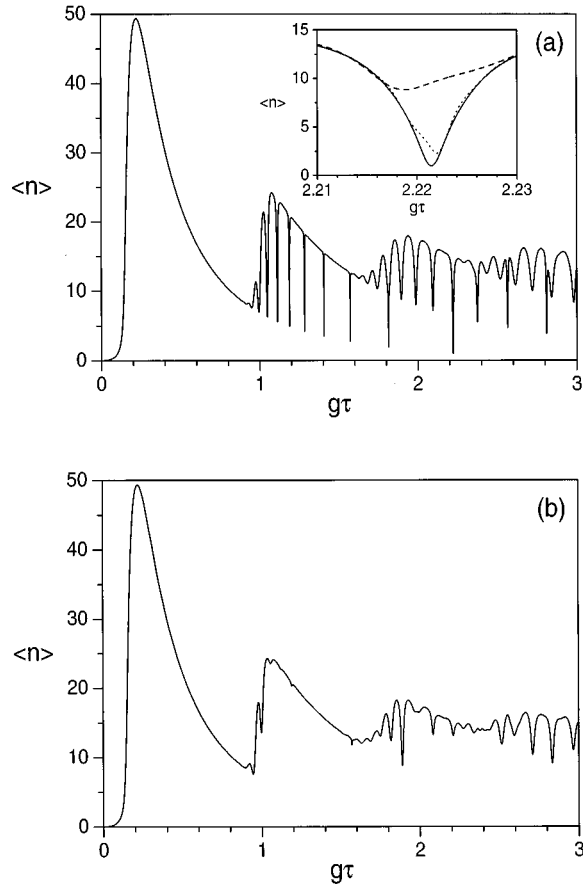


FIG. 4. The mean photon number $\langle n \rangle$ as a function of the interaction time $g\tau$ for the parameters $r/C=50$, $n_b=0$, and (a) $k/\kappa=100$ and (b) $k/\kappa=5$. As shown in the inset, the depths of the trapping resonances decrease for $k/\kappa=20$ (dotted) and $k/\kappa=10$ (dashed).

The trapping resonances occur when for a particular number n of photons in the cavity an initially excited atom undergoes complete Rabi oscillations and leaves the cavity again in the excited state. That is, the probability for depositing a photon has to vanish if the atom finds n photons in the cavity. As seen from the dashed curve in Fig. 3(a), this is no longer the case if the kinetic energy of the atoms is comparable to the atom-field interaction energy.

B. Intermediate regime

If the kinetic energy of the atoms is of the same order as the potential energy, the influence of the potential barrier gets stronger and for $k \approx \kappa_n$ dramatic changes happen. This can be seen in Fig. 5, where $P_{\text{emission}}(0)$ is plotted as a function of k/κ . For $k > \kappa$ Rabi-like oscillations can be seen; for $k < \kappa$ there are oscillations with a much smaller amplitude around a mean value that decreases with decreasing k/κ . In the intermediate regime, we obtain for $k = \kappa_n$ and $\kappa_n L \gg 1$

$$P_{\text{emission}}(n) = \frac{1}{2} \left[1 + \frac{3 \sin^2(\sqrt{2} \kappa_n L)}{8 + \sin^2(\sqrt{2} \kappa_n L)} \right]. \quad (34)$$

As already noted above, a change in the scaling parameter takes place between the Rabi and the mazer limit. To further

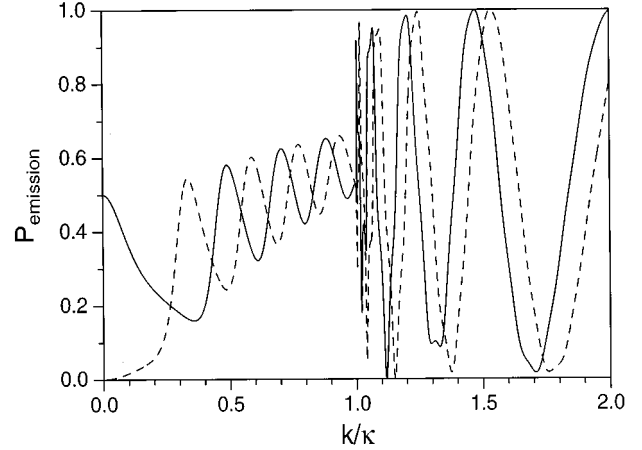


FIG. 5. The emission probability for a mesa potential as a function of k/κ for $\kappa L=10\pi$ (solid curve) and $\kappa L=10.5\pi$ (dashed curve), when the cavity field is initially in the vacuum state.

illustrate this transition, we show the mean photon number in Fig. 6. If $k \approx \kappa$, as shown in Fig. 6(a), there are oscillations in the mean photon number as a function of $g\tau$. For smaller k/κ they become less periodic and their shape less sinelike.

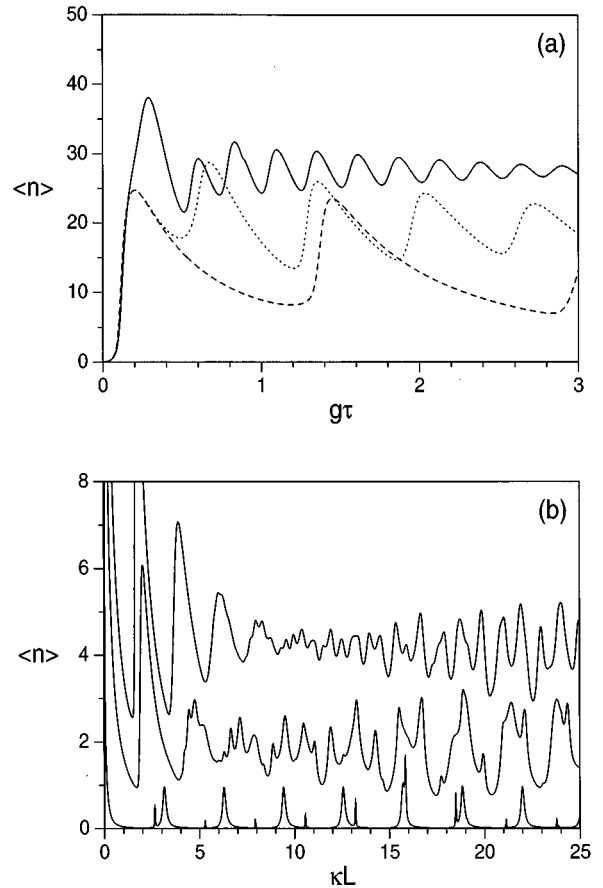


FIG. 6. The mean photon number $\langle n \rangle$ in the intermediate regime vs (a) the interaction time $g\tau$ for $k/\kappa=2$ (solid curve), $k/\kappa=1$ (dotted curve), $k/\kappa=0.5$ (dashed curve) and (b) the interaction length κL for $k/\kappa=0.2, 0.1, 0.01$ (from top to bottom). The other parameters are $r/C=50$ and $n_b=0$.

For $k < \kappa$, the mean photon number becomes more and more periodic if it is plotted as a function of κL , as illustrated in Fig. 6(b). For some parameters in the intermediate regime the mean photon numbers show collapse and revival as a function of κL , for example, in the upper curve in Fig. 6(b). For even slower atoms, the features of collapse and revival become less pronounced and are replaced by an irregular behavior, as exemplified by the middle curve in Fig. 6(b).

C. Mazer limit

For ultracold atoms with $k \ll \kappa_n$, the emission probability is very different. This can already be inferred from the lower curve in Fig. 6(c), whose regular structure should be compared with the irregularity of the middle curve. For the emission probability, we obtain

$$P_{\text{emission}}(n) = \frac{\frac{1}{2} \left[1 + \frac{1}{2} \sin(2\kappa_n L) \right]}{1 + (\kappa_n/2k)^2 \sin^2(\kappa_n L)}. \quad (35)$$

Several aspects of Eq. (35), which is valid for $\kappa L \ll (\kappa/k)^2 \sqrt{n+1}$ and $\exp(\kappa_n L) \gg 1$, should be noted. The emission probability is periodic in $\kappa L \sqrt{n+1}$ instead of $g\tau\sqrt{n+1}$, which is the period in the limit of Rabi oscillations. Equation (35) resembles the Airy function of classical optics, $[1 + F \sin^2(\Delta/2)]^{-1}$, which gives the transmitted intensity in a Fabry-Pérot interferometer with finesse F and total phase difference Δ [14]. In our situation, the finesse is given by $F = (\kappa_n/2k)^2$ and the phase difference by $\Delta = 2\kappa_n L$.

Please note that for very slow atoms the phase difference does not depend on the wavelength of the incoming particles, but on the number of photons in the cavity. This is because the kinetic energy of the atoms that experience the potential well and are transmitted on resonance is inside the cavity only determined by the depth of the potential, since the kinetic energy outside the cavity is very small compared to the atom-field interaction energy.

VI. RESONANCES IN THE MAZER REGIME

A. Without thermal photons ($T=0$)

There are two ways to come to a physical understanding of the quantized- z -motion-induced emission. One of them is based on the reflection and transmission of the dressed-state components, the other one explains the resonances with the picture of de Broglie waves inside the cavity.

Taking Eq. (12) as the basis for an explanation of the quantized- z -motion-induced emission, we first consider the situation where in the absence of thermal photons the cavity field is initially in the vacuum state and the kinetic energy of the incident atoms is assumed to be so small that tunneling through the potential barrier is negligible, i.e., $\rho_n^+ = -1$ and $\tau_n^+ = 0$. Furthermore, $\rho_0^- = -1$ and $\tau_0^- = 0$ when $k \ll \kappa$ so that the atom is reflected and no photon is emitted ($|R_{a0}|^2 = 1$), as in Fig. 7(a). But when $\kappa L = m\pi$ things change drastically: then $\rho_0^+ = -1$ and $\tau_0^+ = 0$ as before, but now $\rho_0^- = 0$ and $\tau_0^- = (-1)^m$, as depicted in Fig. 7(b). Under this resonance condition, the atom is only reflected when it hits the repulsive potential and traverses the cavity when it encounters an

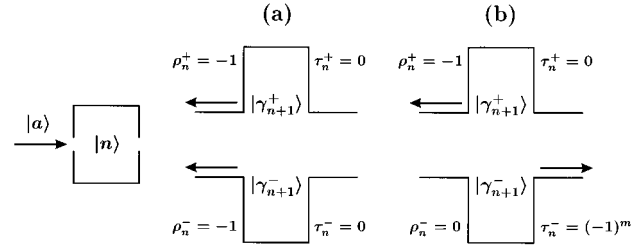


FIG. 7. An excited atom and a cavity field with n photons is described by the state $|a, n\rangle = (|\gamma_{n+1}^+\rangle + |\gamma_{n+1}^-\rangle)/\sqrt{2}$. For very slow incident atoms, the $|\gamma_{n+1}^+\rangle$ component is always reflected by a potential barrier. The $|\gamma_{n+1}^-\rangle$ component, which sees a square-well potential, is reflected for $\kappa L \sqrt{n+1} \neq m\pi$ (a) and is transmitted for $\kappa L \sqrt{n+1} = m\pi$ (b).

attractive potential, in each case emitting a photon half of the time ($|R_{a0}|^2 = |R_{b1}|^2 = |T_{a0}|^2 = |T_{b1}|^2 = 1/4$). Note that 50% of the reflected atoms have deposited a photon in the cavity.

In more physical terms, if the two components of the wave function that are associated with the corresponding repulsive and attractive potentials preserve their relative sign, the internal state of the atom and field does not change, i.e., no photon is emitted. On the other hand, a difference in the reflection or transmission of these components changes the atom-field state and results in the emission of a photon.

It might seem surprising that the reflected atoms can deposit a photon into the cavity with the same probability as the transmitted atoms. In order to understand this, let us consider the atomic CM motion in the cavity. During the interaction with the cavity field, the atoms that are transmitted are faster and the ones that are reflected are slower than outside the cavity. All in all, they spend the same time in the interaction region, as has been pointed out in Ref. [12]. This explains the high probability for reflection with emission.

We now examine the cumulative effect of a sequence of incident excited atoms on a cavity field that is initially in the vacuum state; see Fig. 8. If $\kappa L = m\pi$, the first atom may deposit a photon in the cavity (with probability 1/2). This changes the cavity field, and therefore the potential $V_n^\pm(z)$, which determines the resonance condition; hence the next incident atom is reflected with certainty without emitting a photon (if no photon decays out of the cavity in the meantime). Therefore, in the limit of very slow atoms, at most one photon is in the cavity at a time. The average photon number has to be between zero and one and is determined by the ratio r/C between the injection (or incidence) rate and the cavity decay rate. Figure 9(a) illustrates this behavior for the parameters $k/\kappa = 10^{-3}$ and $r/C = 50$.

With increasing atomic momentum, the finesse F of the emission probability decreases, so that there is a nonvanishing probability of depositing a photon in the cavity even when the resonance condition is not fulfilled. As a consequence, more resonances (corresponding to larger photon numbers) become accessible and can be excited, as shown in Fig. 9. The resonances may occur for particular values of the interaction length, namely, for $\kappa L \sqrt{N} = m\pi$ ($N, m = 1, 2, 3, \dots$). Under this resonance condition, incident

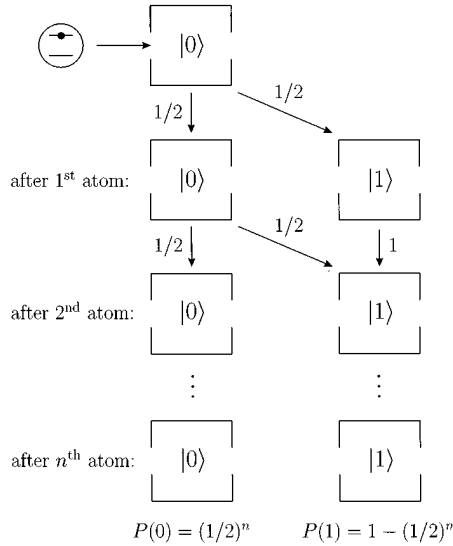


FIG. 8. Schematic diagram showing the cumulative effect of a sequence of very slow excited atoms ($k \ll \kappa$) on a cavity field that is initially in the vacuum state $|0\rangle$. The parameters are such that the resonance condition $\kappa L \sqrt{n+1} = m\pi$ is fulfilled for $n=0$. As a consequence, the emission probability is equal to $1/2$ for $n=0$ and vanishes for $n=1$.

atoms emit a photon with maximal probability if they find $N-1$ photons in the cavity.

For very slow atoms ($k \ll \kappa_n$), one gains further insight by considering the de Broglie wavelength of the atom inside the cavity. The de Broglie wavelength

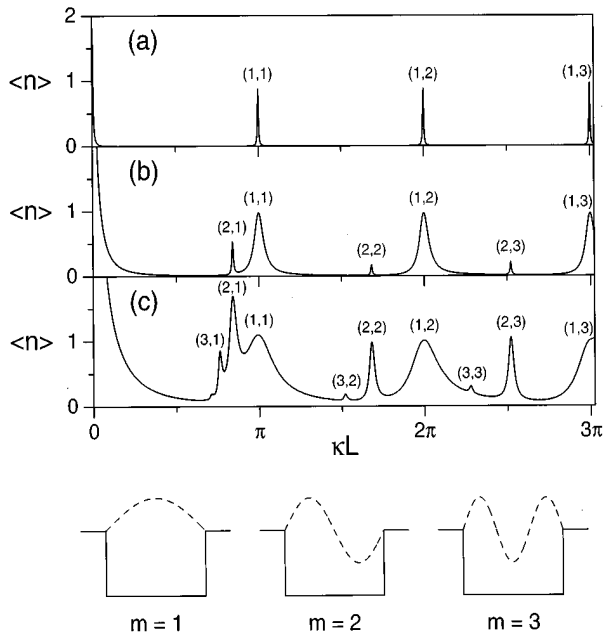


FIG. 9. The mean photon number $\langle n \rangle$ as a function of the interaction length κL for the parameters $r/C=50$, $n_b=0$, and (a) $k/\kappa=0.001$, (b) $k/\kappa=0.01$, and (c) $k/\kappa=0.03$. The peaks are labeled by the pair of integers (N, m) , which appear in the resonance condition $\kappa L^4 \sqrt{N} = m\pi$. The resonances occur when $L = m(\lambda_{dB}/2)$ for the cavity length L and the de Broglie wavelength λ_{dB} inside the cavity.

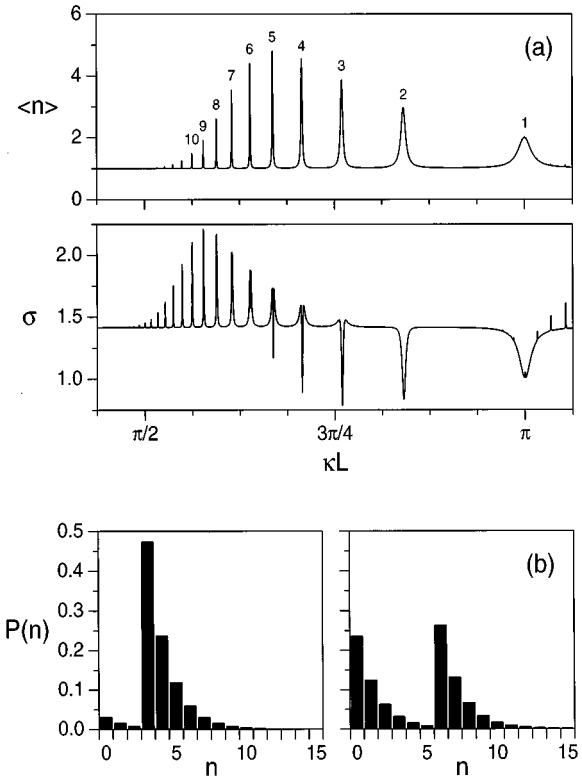


FIG. 10. (a) With thermal photons present, the mean photon number $\langle n \rangle$ and the normalized standard deviation σ show resonances at $\kappa L = \pi/\sqrt[4]{N}$ even for very slow atoms. The peaks are labeled by the integer N . (b) The photon distribution $P(n)$ for $\kappa L = 10^3 \pi^4 / \sqrt{N}$ with $N=3$ (left plot) and $N=6$ (right plot) looks like a pair of thermal distributions one of which is shifted towards larger photon numbers. For all plots, the parameters are $k/\kappa = 10^{-3}$, $r/C = 10^3$, and $n_b = 1$.

$$\lambda_{dB} = \frac{2\pi}{k + \kappa_n} \cong \frac{2\pi}{\kappa^4 \sqrt{n+1}} \quad (36)$$

depends only on the depth of the potential. The resonances in the emission probability occur when the cavity length is an integer multiple of half the de Broglie wavelength, $L = m(\lambda_{dB}/2)$.

B. With thermal photons ($T > 0$)

For very slow atoms and zero temperature of the cavity, only the vacuum resonance (with $N=1$) comes into play. Initial field states with larger photon numbers will be damped until there is at most one photon in the cavity in steady state. In the presence of thermal photons, however, the other resonances may be excited even for very slow atoms ($k \ll \kappa$). This is shown in Fig. 10(a) for the resonance sequence corresponding to $m=1$ and the parameters $k/\kappa = 10^{-3}$, $r/C = 10^3$, and $n_b = 1$. The thermal photons ensure that there is a nonvanishing probability for having different numbers of photons in the cavity, which give rise to different potentials and different resonances.

The peaks in the mean photon number $\langle n \rangle$ are accompanied by resonances in the normalized standard deviation $\sigma = [(\langle n^2 \rangle - \langle n \rangle^2) / \langle n \rangle]^{1/2}$. In Fig. 10(a), the resonances for

$1 \leq N \leq 5$ show reduced photon-number fluctuations as compared to the thermal level $\sigma = (1 + n_b)^{1/2}$, whereas for $N > 5$ the amplitude noise increases.

If the cavity length is adjusted such that the resonance condition $\kappa L^4 \sqrt{N} = m\pi$ is fulfilled for a pair of integers $N = N_0$ and $m = m_0$, then it will also be fulfilled for $N = K^4 N_0$ and $m = K m_0$, i.e., for $N = 16N_0, 81N_0, 256N_0, \dots$. From now on, we always choose N and m such that they are the smallest nonvanishing integers that fulfill the resonance condition.

For $\kappa L = m\pi / \sqrt[4]{N}$ and in the limit $k \ll \kappa$, we obtain from Eqs. (32) and (35) the steady-state photon distribution

$$P(n) = P(0) \left(\frac{n_b}{n_b + 1} \right)^{n-K} \prod_{p=1}^K \frac{n_b + r/2C p^4 N}{n_b + 1} \quad (37)$$

for $K^4 \leq n < (K+1)^4 N$ with $K = 0, 1, 2, \dots$.

If only photon numbers smaller than $16N$ are relevant for the chosen parameters, as was the case in Ref. [6], Eq. (37) can be simplified to give

$$P(n) = \begin{cases} P(0) \left(\frac{n_b}{n_b + 1} \right)^n & \text{for } n < N \\ P(0) \frac{n_b + r/2CN}{n_b + 1} \left(\frac{n_b}{n_b + 1} \right)^{n-1} & \text{for } n \geq N, \end{cases} \quad (38)$$

and the normalization condition $\sum_n P(n) = 1$ implies

$$P(0) = \left[n_b + 1 + \frac{r/C}{2N} \left(\frac{n_b}{n_b + 1} \right)^{N-1} \right]^{-1}. \quad (39)$$

In Fig. 10(b), we plot the photon distributions at the two resonances $\kappa L = 10^3 \pi / \sqrt[4]{N}$ with $N = 3$ and $N = 6$ for $n_b = 1$. Each distribution looks like a pair of thermal distributions one of which is shifted towards larger photon numbers. In general, at the resonance $\kappa L = m\pi / \sqrt[4]{N}$, there is a shift by N photons.

Equations (38) and (39) give the steady-state photon distribution for the mazer with very slow atoms ($k \ll \kappa$) in the presence of thermal photons and for the situation when the resonance condition $\kappa L^4 \sqrt{N} = m\pi$ is fulfilled, that is, we pick κL such that the resonance condition holds for fixed integers N and m . In order to understand why this steady-state distribution looks like a pair of thermal distributions, we consider an initial thermal distribution $P_0(n)$ with $\langle n \rangle = n_b$ as in Fig. 11(a); this is the steady-state solution in the absence of the pumping atoms. A very slow excited incident atom will only emit a photon into the cavity (with probability 1/2) if it encounters $N-1$ photons in the cavity; in all other cases, the emission probability is in general negligible. Thus, whenever there are $N-1$ photons in the cavity, there is a large probability for an incident excited atom to deposit an additional photon, thereby increasing the probability for having N photons in the cavity and decreasing $P(N-1)$. Without the interaction with the thermal reservoir (or for a very small cavity decay rate), we would find after the passage of many atoms the following photon distribution: $P(N-1) \cong 0$, $P(N) \cong P_0(N-1) + P_0(N)$, and $P(n) = P_0(n)$ for all $n \neq N-1, N$. The interaction with the thermal bath leads to

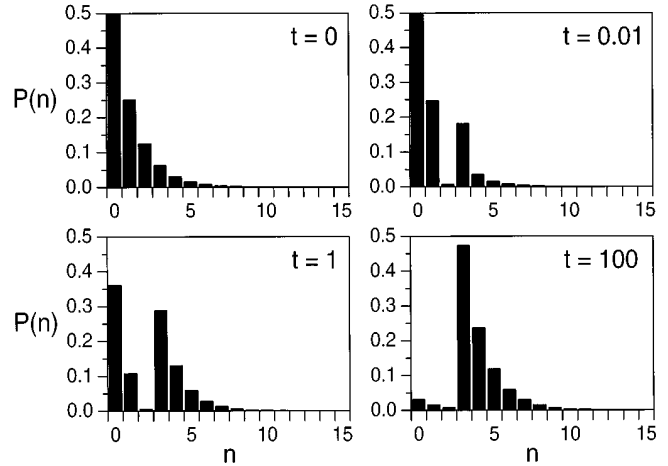


FIG. 11. Time evolution of the photon distribution $P(n)$ for the parameters $\kappa L = 10^3 \pi / \sqrt[4]{N}$ with $N = 3$ and $k/\kappa = 10^{-3}$, $r/C = 10^3$, and $n_b = 1$ from an initial thermal distribution with $\langle n \rangle = 1$ at $t = 0$, $t = 0.01C^{-1}$, $t = C^{-1}$, and $t = 100C^{-1}$.

cavity damping and provides thermal photons, thereby ensuring that the ratio $P(n+1)/P(n)$ approaches its thermal-equilibrium value $n_b/(n_b + 1)$ for all n except for $n = N-1$ where we have a steep increase of the ratio due to the pumping by the incident atoms, $P(N)/P(N-1) = (n_b + r/2CN)/(n_b + 1)$, as can be seen from Eq. (38). The smaller the cavity decay rate and the larger the pump rate (and the ratio $r/2CN$), the larger the ratio $P(N)/P(N-1)$. This explains the photon distributions of Figs. 11 and 10(b).

Moreover, as seen from the expression (39) for $P(0)$, the probability for finding fewer than N photons in the cavity can be suppressed by increasing r/C so that the resulting photon distribution is a shifted thermal distribution. Shifting a distribution to larger photon numbers does not change its variance. The normalized standard deviation, however, is decreased since the mean is increased. Thus, for small N and large r/C , the photon distribution may even be sub-Poissonian ($\sigma < 1$). This is the case in the left plot of Fig. 10(b), where $\sigma \cong 0.81$.

If we consider larger cavity temperatures with more thermal photons present, we obtain not only a pair of thermal distributions, but a whole sequence. This is shown in Fig. 12, which displays a distribution we call ‘‘dragon.’’ In addition to the peaks at $n = 1$, $n = 2^4$, and $n = 3^4$, there is an ‘‘accidental’’ peak at $n = 39$, since $\kappa L^4 \sqrt[4]{39}/\pi = 10^3 \sqrt[4]{39}$ differs only by 0.0006 from an integer.

VII. SINUSOIDAL POTENTIAL AS AN ATOMIC MIRROR

When the cavity mode is described by a sinusoidal mode function as in a TE mode instead of the mesa function (13), which describes a TM mode, the reflection and transmission coefficients change and the emission probability is modified. The coefficients can be calculated in the Wentzel-Kramers-Brillouin (WKB) approximation; details of the calculation will be given in Ref. [10].

We consider the sinusoidal mode function

$$u(z) = \begin{cases} \sin(2\pi z/L) & \text{for } 0 < z < L \\ 0 & \text{elsewhere.} \end{cases} \quad (40)$$

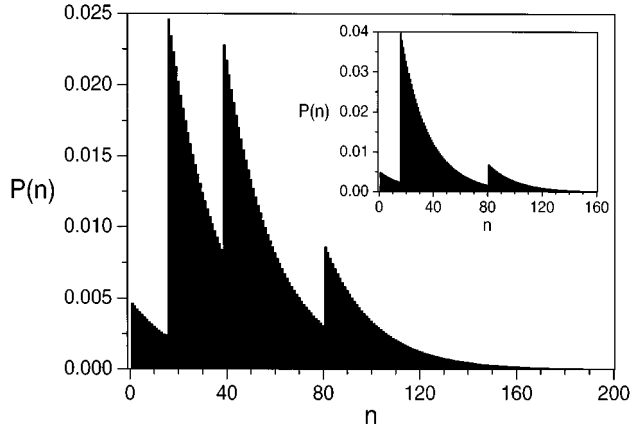


FIG. 12. The photon distribution $P(n)$ for the parameters $k/\kappa = 10^{-3}$, $n_b = 20$, $r/C = 10^4$, and $\kappa L = 10^3 \pi$ ($\kappa L = \pi$ for the inset).

For large values of L and $k < \kappa_n$, we obtain the reflection and transmission coefficients

$$\begin{aligned} \rho_n^\pm &= -i \exp(2i \phi_n^\pm), \\ \tau_n^\pm &= 0. \end{aligned} \quad (41)$$

Analytical expressions for the phase integrals

$$\begin{aligned} \phi_n^+ &= \int_0^{z_0} \sqrt{k^2 - \kappa_n^2 u(z)} dz, \\ \phi_n^- &= \int_0^{L/2} \sqrt{k^2 + \kappa_n^2 u(z)} dz + \phi_n^+, \end{aligned} \quad (42)$$

where $z_0 = (L/2\pi) \arcsin(k^2/\kappa_n^2)$, are given in Ref. [10].

The incident atom is always reflected. Half of the time, it encounters immediately a potential barrier and is reflected. However, when it first encounters the attractive part of the sinusoidal potential, the atomic wave function can pick up an additional phase before the atom is reflected off the repulsive part of the potential. This additional phase varies with the length of the cavity and gives rise to the emission probability

$$P_{\text{emission}}(n) = \sin^2(\Delta_n) \quad (43)$$

with the phase difference $\Delta_n = \phi_n^- - \phi_n^+$.

The incident excited atoms deposit a photon in the cavity with a fixed probability, which can take on any value between zero and one, depending on the length of the cavity. In particular, the cavity length can be such that all the atoms deposit a photon into the cavity while they are reflected. The cavity field acts as a mirror that may or may not change the internal state of the incident atoms in addition to reflecting them. State-changing and state-preserving mirrors for atoms can be built.

VIII. SUMMARY

We have considered a micromaser pumped by slow atoms. If the kinetic energy of the atoms is comparable to the atom-field interaction energy, effects of the quantum-mechanical CM motion become important. In this regime, the emission probability and the photon statistics change dramatically, as compared to the usual maser. We have derived the quantum theory of the maser and given exact analytical results for a mesa mode function. Sharp resonances occur in the emission probability as a function of the interaction length, when the de Broglie wavelength of the atoms fits into the cavity. As a result of the cumulative effect of several incident atoms, unusual photon distributions are obtained. In the case of a sinusoidal potential, the cavity field can act as a state-preserving or state-changing mirror for the incident atoms.

With the rapid progress in the cooling and manipulation of single atoms, an experimental demonstration of the quantized- z -motion-induced emission, e.g., by detecting reflected atoms that have deposited a photon in the cavity, seems to be feasible. In a first experiment, the cavity potential could be enhanced by an injected field. A more detailed discussion of experimental parameters and setups together with the study of smooth mode functions will be given in Ref. [10].

ACKNOWLEDGMENTS

This work has been supported by the Office of Naval Research, the Welch Foundation, and the Texas Advanced Research Program.

[1] For a review of early work on Rydberg atoms in microwave cavities, see S. Haroche and J. M. Raimond, *Adv. At. Mol. Phys.* **20**, 350 (1985).
 [2] The first realization of a micromaser was reported in D. Meschede, H. Walther, and G. Müller, *Phys. Rev. Lett.* **54**, 551 (1985).
 [3] P. Filipowicz, J. Javanainen, and P. Meystre, *Phys. Rev. A* **34**, 3077 (1986).
 [4] L. A. Lugiato, M. O. Scully, and H. Walther, *Phys. Rev. A* **36**, 740 (1987).
 [5] A recent review is given by G. Raithel, C. Wagner, H. Walther, L. M. Narducci, and M. O. Scully, in *Cavity Quan-*

tum Electrodynamics, edited by P. R. Berman (Academic, Boston, 1994), p. 57.
 [6] M. O. Scully, G. M. Meyer, and H. Walther, *Phys. Rev. Lett.* **76**, 4144 (1996).
 [7] Laser-cooling techniques are reviewed in *Laser Manipulation of Atoms and Ions*, edited by E. Arimondo, W. D. Phillips, and F. Strumia (North-Holland, Amsterdam, 1992).
 [8] B.-G. Englert, J. Schwinger, A. O. Barut, and M. O. Scully, *Europhys. Lett.* **14**, 25 (1991).
 [9] S. Haroche, M. Brune, and J. M. Raimond, *Europhys. Lett.* **14**, 19 (1991).
 [10] M. Löffler, G. M. Meyer, M. Schröder, M. O. Scully, and H.

- Walther, paper II, Phys. Rev. A **56**, 4153 (1997).
- [11] M. Schröder, K. Vogel, W. P. Schleich, M. O. Scully, and H. Walther, paper III, Phys. Rev. A **56**, 4164 (1997).
- [12] The influence of field damping during the atom-field interaction has been studied for a single atom in M. Battocletti and B.-G. Englert, J. Phys. II **4**, 1939 (1994).
- [13] P. Meystre, G. Rempe, and H. Walther, Opt. Lett. **13**, 1078 (1988).
- [14] See, for example, M. Born and E. Wolf, *Principles of Optics* (Macmillan, New York, 1959).